Urban Climate 14 (2015) 176–186

Contents lists available at ScienceDirect

Urban Climate

journal homepage: www.elsevier.com/locate/uclim

Spatial variation of the daytime Surface Urban Cool Island during the dry season in Erbil, Iraqi Kurdistan, from Landsat 8

Azad Rasul [a,b,*], Heiko Balzter [a,c], Claire Smith [a]

[a] University of Leicester, Centre for Landscape and Climate Research, Department of Geography, University Road, Leicester LE1 7RH, UK
[b] Soran University, Department of Geography, Soran, Erbil, Iraq
[c] National Centre for Earth Observation, University of Leicester, University Road, Leicester LE1 7RH, UK

ARTICLE INFO

Article history:
Received 16 May 2015
Revised 19 June 2015
Accepted 9 September 2015

Keywords:
Surface Urban Cool Island (SUCI)
Urban Heat Island (UHI)
Urban climate
Surface temperature
Erbil
Remote sensing

ABSTRACT

Differences between the energy balance of cities and their non-urban surroundings exist due to modification of surface properties. In temperate and sub-tropical climates, these differences are manifest as the Urban Heat Island (UHI) effect. However in more arid environments man-made modifications of the environment can cause urban cooling relative to the surrounding landscape particularly during the dry season. This research examines the spatial formation of the daytime Surface Urban Cool Island (SUCI) effect of Erbil city in Iraq, as a case study of cities in semi-arid climates. Six satellite images acquired by Landsat 8 during the period from 1st July to 19th September 2013 are used to retrieve Land Surface Temperature (LST), identify Land Use/Land Cover (LULC) classes and investigate the spatial variation of LST and the SUCI intensity. In order to find out the key drivers of the observed patterns of LST, the relationship with wetness, brightness, bareness, built-up and vegetation index maps are examined. The results indicate that densely built-up areas, such as central districts of the city, green areas and water bodies, had lower LST acting as cool islands, compared to the non-urbanized area around the city. In contrast, the airport, open spaces and new low-density housing developments on the outskirts of the city, experienced higher LST and showed an SUHI effect. A very strong inverse relationship is evident between surface temperature and wetness index ($r = -0.9$; $p < 0.01$). A strong positive correlation ($r = 0.75$; $p < 0.00001$) is apparent with the brightness index. In contrast, between surface temperature and the greenness index a moderate negative correlation was found ($r = -0.39$; $p < 0.01$) for a typical dry season day. The results show that during the daytime residential areas in the city centre recorded an LST of 46.2 ± 1.74 °C. Urban Cool Island Intensity (UCII) of the city ranged from 3.5 to 4.6 °C compared to a 10 km buffer zone around the city. This study shows that during the dry season in some cities, such as Erbil, the surface wetness is the main determinant of the UCI effect, and not vegetation cover.

1. Introduction

The difference between the characteristics of surface cover in urban and non-urbanized areas in terms of 3-d geometry of the built area, heat absorption, the building materials, surface albedo and amount of vegetation lead to different air and

* Corresponding author at: University of Leicester, Centre for Landscape and Climate Research, Department of Geography, University Road, Leicester LE1 7RH, UK.
E-mail address: aor4@le.ac.uk (A. Rasul).

http://dx.doi.org/10.1016/j.uclim.2015.09.001
2212-0955/

surface temperatures within a city relative to the surrounding area. Therefore, urban expansion can lead to radical changes in the nature of the surface of the urbanized area. Usually, this urban extension causes temperatures to increase in temperate and sub-tropical climates, a phenomenon known as the Urban Heat Island (UHI) effect (Oke, 1987; Weng et al., 2004; Farina, 2011). In contrast, built-up areas in semi-arid regions have been found to exhibit lower surface temperatures compared to non-urbanized dry surroundings (Frey et al.; Cai and Du, 2009; Shigeta et al., 2009), which has been termed the Urban Cool Island (UCI) effect.

Satellite sensors can be used to obtain the surface temperature of urban areas and to study the spatial variations of UHIs and their development (Watson, 2012). Rao (1972) reported the first study of Surface Urban Heat Island (SUHI) based on satellite imagery. He used thermal Infrared Radiometer (IR) data of the Improved TIROS Operational Satellite (ITOS-1) to study the; surface temperature patterns of the mid-Atlantic coast. Subsequently, Matson et al. (1978) detected the night-time UHI of the Midwestern and Northwestern United States from NOAA 5 satellite data. The UHI of the New York City/New England area was also detected by Price (1979). Since then, SUHIs and surface temperatures have been observed from different platforms including satellites, aircraft and ground-based sensors. Landsat TM and ETM+ are widely used to investigate the expansion of SUHIs and to assess the relationship between Land Surface Temperature (LST) and Land Use/Land Cover (LULC) (e.g. (Xu, 2009; Li et al., 2011; Ukwattage and Dayawansa, 2012).

It is notable that very few investigations of the SUHI/SUCI effect in arid environments have been published. One exception is the study by Lazzarini et al. (2013) who used MODIS data to analyse daily differences of LST and UHI in Abu Dhabi. Their findings indicate the presence of a standard nocturnal UHI, in contrast to a daytime UCI. The amount of soil moisture within the urban area has an effect on the thermal environment because evaporation reduces land surface temperature via latent cooling. As such, the Lazzarini study demonstrated the existence of a UCI in Dubai compared with the surrounding desert; both residential districts and industrial areas had lower temperatures than sand zones (Frey et al.; Frey et al., 2006).

The correlation between LST and Normalized Difference Vegetation Index (NDVI) values has been applied extensively in UHI studies (Weng et al., 2004; Sun and Kafatos, 2007; Weng and Lu, 2008; Schwarz et al., 2012). The existence of a strong linear inverse relationship was confirmed by Liang and Shi (2009) and Bajaj et al. (2012). On the contrary, Zhang et al. (2008) referred to the absence in the relationship between LST and NDVI in Shanghai, China. Similarly, Yuan and Bauer (2007) confirmed that this relationship suffers from clear seasonal variations. In order to examine the relationship between air UHI and surface UHI, atmospheric temperature and LST data have been combined by several researchers (e.g. Gallo and Owen, 1999; Voogt and Oke, 2003; Hartz et al., 2006). A strong relationship has been found between the air and LSTs in Leipzig city in Germany, in relation to the UHI effect (Schwarz et al., 2012).

Early research used a Tasselled Cap to extract parameters from the Multispectral Scanner Sensor (MSS) of Landsat 1 (Kauth and Thomas, 1976). This method has subsequently been widely applied, because in addition to the collection of multiple measurements in different bands it shows the physical properties of the scene (Liu et al., 2014).

Chen et al. (2006) used a range of indices (Normalized Difference Bareness Index (NDBaI), Normalized Difference Built-up Index (NDBI), NDVI and Normalized Difference Water Index (NDWI)), to examine the relationship between UHI and LULC changes. In this study we use NDVI and NDBI to examine how they influence the SUCI intensity in a semi-arid environment.

Research on the UCI effect is still in its infancy (Li et al., 2011) and its characteristics in semi-arid environments still need to be better quantified and understood. The objective of this study is to quantify the spatial structure of the SUCI in Erbil, as a case study of a semi-arid climate and to establish the key determinant factors and patterns of the spatial distribution of LST and SUCI. The contribution and novelty of this paper is:

- Determination of the spatial distribution of the patterns of LST and SUCI in the different LULC and districts of the city of Erbil.
- Using wetness, brightness and greenness components derived from Landsat OLI by Tasselled Cap transformation (TCT), to find key factors responsible for the spatial LST variation.

1.1. Study area

Erbil is the capital city of the Kurdistan Region of Iraq. The city is located in northern Iraq and lies between 36°08′N to 36°14′N, and 43°57′E to 44°03′E. (Fig. 1). It is located 412 m above sea level (Sharif, 1998).

In 2010, the estimated population of Erbil Governorate was 1,820,000, whilst the population in the city was 852,000 (KRSO, 2012). The population density of Erbil district is 472.9 (persons/km^2) (Amjed et al.). The city has experienced extensive growth over the past two decades, both in terms of population and infrastructure.

Erbil is selected as a case study located within a semi-arid and continental climate. According to the Köppen climate classification, the city is tropical/subtropical semiarid (BSh) (Hasan, 2006). It experiences cool, rainy winters and warm, dry summers. The average annual temperature and precipitation of Erbil is 21.85 °C and 386 mm, respectively (Meteorological and Seismological Department of Erbil Governorate, 2014). July and August are the hottest months of the year; air temperatures during these months can reach 49 °C. Usually, summer months are dry; the majority of the year's precipitation falls between March and December.

Land use/land cover are strongly dependent on the seasonality of the precipitation, hence winter grain cultivation such as wheat and barley is common in rural areas. Inside the city, residential land use is most dominant. The residential buildings are usually block and concrete.

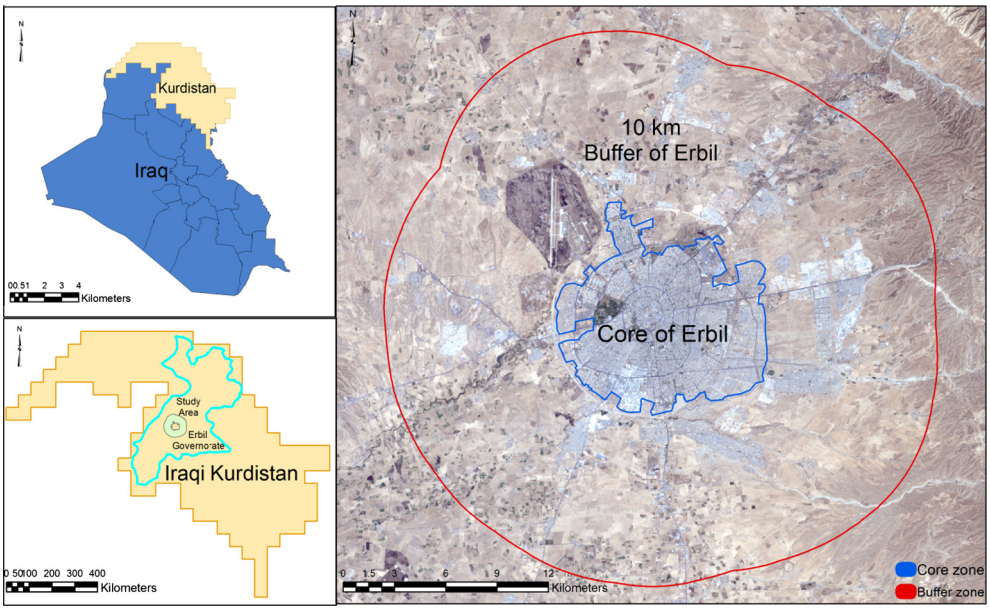

Fig. 1. map of Iraq, Kurdistan Region and true colour Landsat of the study area.

2. Data and methodology

2.1. Data and pre-processing

Land surface temperature data are extracted from six Thermal Infrared Radiometer images acquired by Landsat TIRS (Landsat 8) from 1st July to 19th September 2013 (Table 1). These are used to retrieve land surface temperature (Path 169, Row 035). The images are level L1T data and were captured under clear atmospheric conditions (<1 % cloud coverage). These images were provided by the United States Geological Survey (USGS), Earth Explorer website (http://earthexplorer.usgs.gov/).

A composite image of summer time Landsat 8 is produced by calculating the pixel-based mean of all of the six images for the thermal and OLI bands. This composite image is used for all of the subsequent analysis. For the thermal bands of Landsat 8, thermal atmospheric correction was applied because it has two thermal channels. Furthermore, Quick Atmospheric Correction (QUAC) is appropriate for atmospheric corrections of OLI Bands of Landsat OLI.

Shapefiles of LULC were created based on a true colour image from Landsat 8. Digital Globe imagery with 0.5 m resolution was acquired on 5th July 2010 and a map of Erbil's districts was prepared by the GIS Centre of Erbil Governorate. Exemplar LULC classes were selected based on expert knowledge to assess how LST varied according to LULC (Fig. 2). These were comprised of 'Commercial Areas', 'Industrial', 'Airport', 'Compact low-rise LCZ 3', 'Sparsely built LCZ 9', 'Bare soil LCZ F', 'Dense trees LCZ A', 'Scattered trees LCZ B' 'Grass' and 'Water'(Stewart and Oke, 2012).

A map of the districts of Erbil was prepared based on Open Street Map data and the map of Erbil's districts. The digitized district boundary map was georeferenced, projected to WGS-1984 UTM zone 38N. Minimum, maximum and mean LST were calculated for each district with the Zonal Statistics Tool in ArcMap.

2.2. Retrieval of LST

The digital number of Landsat TIRS was converted to at-sensor radiance, using Eq. (1) (USGS, 2013).

Table 1
Images used in this study.

Number	Date	Time	Cloud cover (%)	Image quality	Path/raw	Spatial resolution (m)
1	01/07/2013	07:40:58	0.01	9	169/35	30 OLI/100 TIRS
2	17/07/2013	07:40:58	0.01	9	169/35	30 OLI/100 TIRS
3	02/08/2013	07:41:00	0.02	9	169/35	30 OLI/100 TIRS
4	18/08/2013	07:41:01	0.01	9	169/35	30 OLI/100 TIRS
5	03/09/2013	07:41:02	0.03	9	169/35	30 OLI/100 TIRS
6	19/09/2013	07:40:57	0.72	9	169/35	30 OLI/100 TIRS

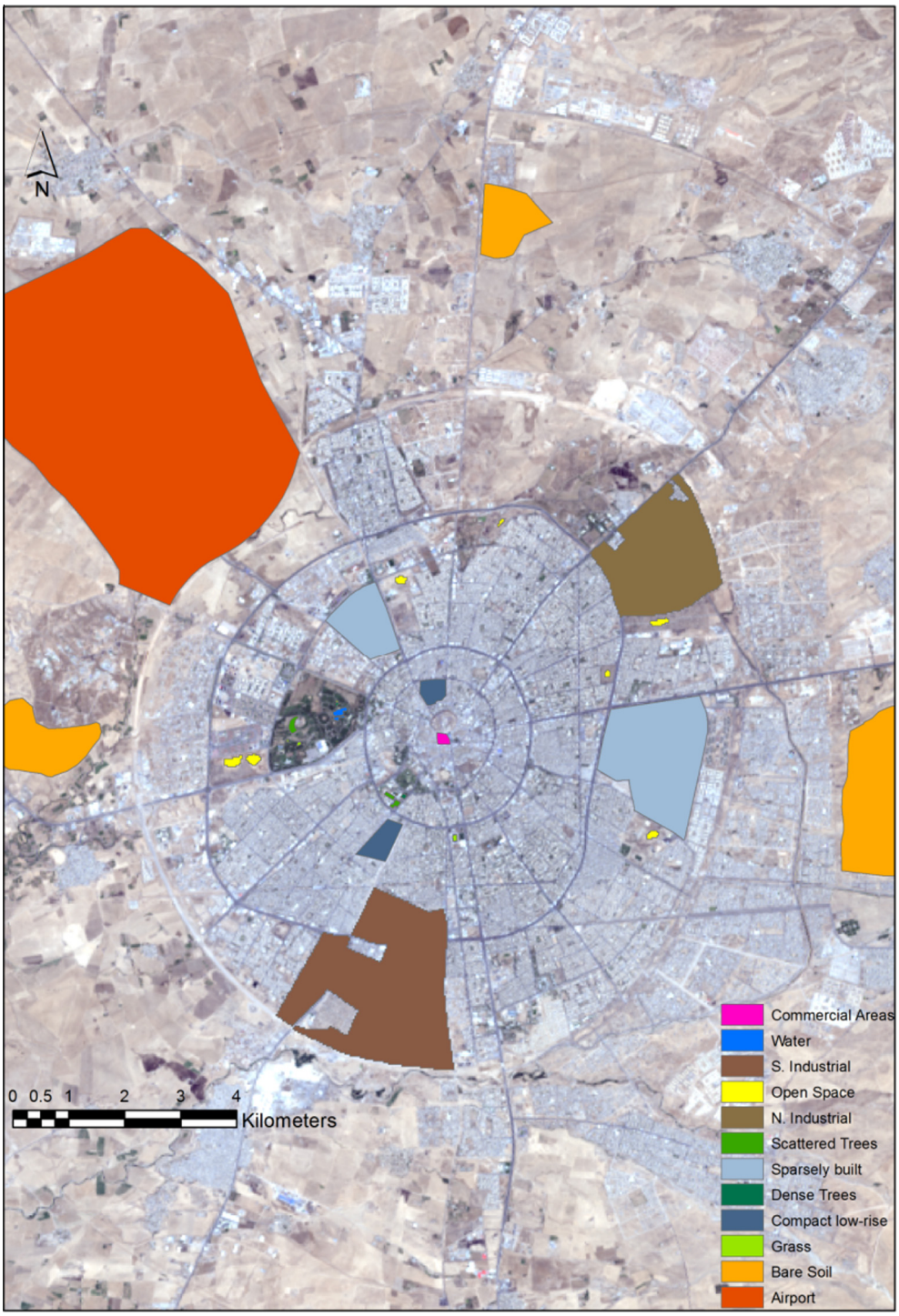

Fig. 2. samples of selected LULC with the true colour Landsat OLI.

$$L_\lambda = \text{gain} * \text{DN} + \text{offset} \quad (1)$$

where L_λ = at-sensor spectral radiance (W/(m^2 srad μm)); gain = (0.0003342) rescaling factor specific to each band from the metadata. Offset = (0.1) rescaling factor added to each band from the metadata. DN = digital number of a given pixel.

These values were subsequently converted to at-satellite brightness temperature with Eq. (2):

$$\mathrm{TB} = \frac{k_2}{\ln\left(\frac{k_1}{L_\lambda} + 1\right)} \tag{2}$$

where TB = brightness temperature in Kelvin, $k_1 = 774.89$ and $k_2 = 1321.08$ are calibration constants from the metadata (USGS, 2013).

2.2.1. Emissivity correction

An emissivity correction is required to accurately derive LST from satellite imagery (Srivastava et al., 2009).

The Emissivity Normalisation Method was applied here. It was first described by Gillespie (1986) and has also been recommended by Li et al. (1999) to calculate emissivity. The approach calculates the emissivity of the highest temperature for each pixel (Zhang et al., 2008; Li et al., 2013). Eq. (3) is then used to correct surface emissivity (Zhang et al., 2013).

$$T_s = \frac{\mathrm{TB}}{(1 + (\lambda \mathrm{TB}/\rho)\ln\varepsilon)} \tag{3}$$

where T_s is land surface temperature (in Kelvin); TB is radiant surface temperature (in Kelvin); λ is the wavelength of emitted radiance (11.5 μm); ρ is $h \times c/\sigma$ (1.438×10^{-2} m K); h is Planck's constant (6.26×10^{-34} J s); c is the velocity of light (2.998×108 m/s); σ is Stefan Boltzmann's constant (1.38×10^{-23} J K^{-1}); and ε is emissivity (Farina, 2011).

2.3. Identification of the surface UCI and UHI intensity

Surface UCII and UHII is the difference between the surface temperature of an urban area and its rural surroundings (Stathopoulou and Cartalis, 2007). There is no standardised method of measuring UHII. A ten kilometre buffer zone around Erbil city is used here to define the reference 'rural' surface temperature. In this study, the magnitude of both SUCI and SUHI is calculated by Eqs. (4) and (5) (Oke, 1987; Li et al., 2011).

$$\mathrm{SUHI} = T_u - T_r \tag{4}$$

$$\mathrm{SUCI} = T_r - T_u \tag{5}$$

where SUHI = Surface Urban Heat Island. SUCI = Surface Urban Cool Island. T_u = mean LST of Urban or Core. T_r = mean LST of Rural Buffer.

2.4. Calculating wetness, greenness and brightness components

One of the advantages of the Tasselled Cap Transformation (TCT) is the ability to consolidate spectral data into a few bands with little loss of information (Baig et al., 2014). The most relevant indicators for the current study, which can be acquired using TCT the obtained from Landsat 8, are brightness, greenness and wetness. The first feature is a brightness index which is a weighted sum of all reflective (OLI) bands. It is related to bare or semi bare soil, natural and artificial features. Greenness is characterised by a high absorption in visible bands and high reflectance in the near band. The greenness index significantly correlates with leaf index and healthy biomass, whilst it is proven that wetness is sensitive to soil and plant moisture (Crist and Cicone, 1984; Jin and Sader, 2005; Baig et al., 2014). The Brightness Indices (BI), Greenness (GVI) and Wetness (WI) are calculated using Eqs. (6), (7) and (8), respectively (Baig et al., 2014).

$$\mathrm{BI} = (.3029 * b2) + (.2786 * b3) + (.4733 * b4) + (.5599 * b5) + (.508 * b6) + (.1872 * b7) \tag{6}$$

$$\mathrm{GVI} = (-.2941 * b2) + (-.243 * b3) + (-.5424 * b4) + (.7276 * b5) + (.0713 * b6) + (-.1608 * b7) \tag{7}$$

$$\mathrm{WI} = (.1511 * b2) + (.1973 * b3) + (.3283 * b4) + (.3407 * b5) + (-.7117 * b6) + (-.4559 * b7) \tag{8}$$

where: BI = brightness index, GVI = greenness index, WI = wetness index. b2–b7 = digital number of bands 2–7.

Consequently, a few extreme values of the results of each of the Tasselled Cap components replaced with the replace bad value tool in ENVI software and then they are rescaled to [1,100].

2.5. Calculating built-up and vegetation indices

NDBI was proposed by Zha et al. (2003) as a sensitive indicator of built up area. They used this index to map the built-up area of Nanjing city in the east of China. In this example, the study area has a humid, subtropical climate and the index provided high accuracy due to the vegetated and wet surroundings; the index has limitations in built-up areas located in barren regions due to the similarity of the spectral properties in all TM bands. NDBI was calculated by using Eq. (9) (Zha et al., 2003).

$$\mathrm{NDBI} = \frac{(\rho_{MIR} - \rho_{NIR})}{(\rho_{MIR} + \rho_{NIR})} \tag{9}$$

where: NDBI = Normalized Difference Built-up Index, ρ_{MIR} is the surface reflectance of Mid Infrared band (6), and ρ_{NIR} is the surface reflectance of Near Infrared band (5) in Landsat OLI.

The simple and widely used vegetation index is NDVI. Compared to NDVI, GVI is a multiple linear spectral combination (e.g. four bands for MSS and six bands for TM, ETM+ and OLI) and it is a type of data transformation used to distinguish healthy vegetation. In contrast, NDVI is a ratio based index using two bands (red and near infrared) to identify healthy vegetation and green biomass changes. Both of these indices rely on the fact that vegetation has a strong absorption in the red band and a strong reflection of the radiation in the NIR band (Karnieli et al., 2010; Wu, 2014). Aufmuth (2001) concluded that GVI and NDVI are well correlated whereas Todd et al. (1998) found that when the vegetation cover is low, GVI was less affected by moisture content and soil type. To calculate NDVI, Sobrino's equation was employed (Sobrino et al., 2004) Eq. (10).

$$\mathrm{NDVI} = \frac{(\rho_{NIR} - \rho_{RED})}{(\rho_{NIR} + \rho_{RED})} \tag{10}$$

where: NDVI = Normalized Difference Vegetation index, ρ_{NIR} is the surface reflectance of band 5, and ρ_{RED} is the surface reflectance of band 4 in Landsat OLI.

3. Results and discussions

3.1. UCI in the city

The spatial distribution of LST indicates significant differences between the urban thermal environment and its surroundings. The mean LST inside the city was 46.2 ± 1.74 °C, compared to a mean LST of 50.1 ± 1.76 °C in the10 km buffer zone surrounding the city. The UCII of the city ranges from 3.5 to 4.6 °C (Table 2).

3.2. Variation of LST with land use/land cover

The influence of land cover on LST and SUHII was assessed by calculating zonal statistics. Fig. 3 indicates that water bodies (Lake 1 and Lake 2) have the lowest average LST (40.22 ± 1.59 °C), as would be expected (e.g. (Frey et al.; Stathopoulou and Cartalis, 2007). The highest mean LSTs are found at the Airport (53.11 ± 2.6 °C) and within the Barren Land category (50.93 ± 0.49 °C). The mean surface temperatures for North Industrial and South Industrial areas are 48.1 ± 1.57 and 46.67 ± 1.54 °C, respectively. The cooling influence of vegetation is apparent from the cooler surface temperatures found in the more vegetated zones of dense trees (42.8 ± 1.91 °C) and grasses (43.86 ± 2.46 °C).

3.3. Variation of SUCI and SUHI in selected LULC classes

The magnitude of the SUHII/SUCII varies considerably between LULC categories (Fig. 3). Relative warming (compared to the buffer zone) of 3.01 °C is associated with the Airport class. Warming was also exhibited in the Bare Soil (0.83 °C) and Open Area (0.4 °C) classes. This warming is due to low soil moisture and limited tree and other plant cover in these areas. In contrast, a surface urban cool island was evident in all other land cover types. The greatest SUCI intensity is 9.88 °C found at the artificial lakes within the Sami Abdurrahman Park compared to the mean LST of the buffer of the city at the same time. Green areas experienced a significant decrease of temperature compared to the mean temperature of the city. The SUCI intensity values of Dense Trees and Grass is 7.3 and 6.24 °C, respectively. The main reasons for this difference are the low heat storage capacity and heat losses through evaporation and transpiration processes in the green areas.

3.4. Spatial variation of wetness, brightness and greenness components

Wetness, brightness and greenness were calculated for the study area using the Tasselled Cap (Baig et al., 2014). The highest values of wetness were found in the Water and Dense trees classes, whilst Bare Soil and Open Space experienced the lowest wetness. The mean wetness of Water was 54.67 ± 9.84 and the mean wetness of Dense Trees was 47.69 ± 6.2. However, Bare Soil and Open Space recorded 7.54 ± 4.4 and 15.09 ± 6.74, respectively (Fig. 4). This low wetness and soil moisture in Bare Soil and Open Space is the main reason for the increased LST in the buffer zone and Sparsely Built areas. The Grass and Dense Trees classes showed the highest greenness meanwhile the South Industrial and Commercial areas experienced the lowest greenness. The greenness of Grass is 61.51 ± 13.81 whilst the greenness of Commercial was 17.63 ± 1.69. In terms of brightness, Bare Soil and Open Space showed the highest brightness whilst Water and Dense trees experienced the lowest

Table 2
Land surface temperature in Erbil and its surroundings during summer 2013.

Area	Min LST (°C)	Max LST (°C)	Mean LST (°C)	SD LST (°C)
Core (city)	34.1	53.5	46.2	1.74
Buffer (10 km)	37.6	58.1	50.1	1.76

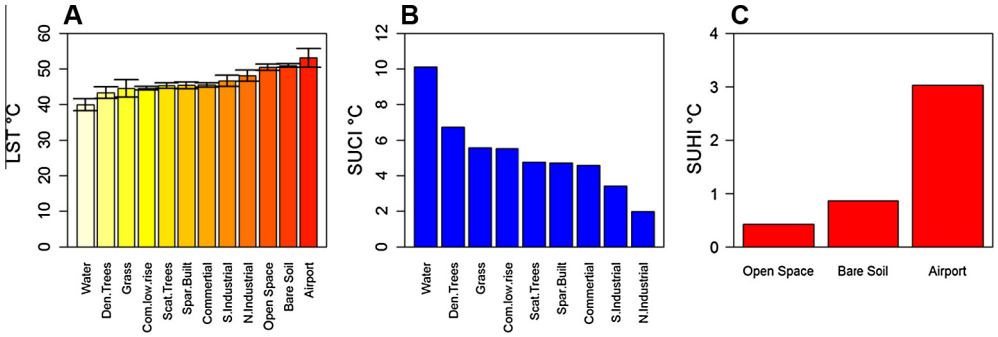

Fig. 3. Mean LST, SUCI and SUHI in the LULC classes during summer 2013.

wetness. Brightness of both Bare Soil and Open Space is 79.9 ± 2.84 and 75.05 ± 6.17, whilst the brightness of the Water and High Density Tree classes was 49.74 ± 12.11 and 58.95 ± 5.96, respectively.

The wetness of the city centre is 27.39 ± 8.29 whilst the buffer is less wet (15.49 ± 6.8). The main factor explaining the decrease of LST in the city is higher soil moisture. In terms of brightness, the buffer of the city is brighter (77.32 ± 6.08) and the mean brightness of the city is 69.14 ± 5.93. Generally, vegetation in the study area in the summer is low. The mean greenness of the city is 23.23 ± 7.52 and the buffer is more greenness (28.93 ± 5.29).

3.5. Relationship between land surface temperature and wetness, brightness and greenness in different LULC classes

3.5.1. Surface temperature and wetness

The wetness factor, which refers to the amount of soil moisture, corresponds well with the spatial distribution of surface temperature in the case study area. The relationship between LST and wetness index shows a very strong inverse relationship (Fig. 5, $r = -0.9$, $p < 0.01$). This means that as the wetness index increases the LST will decrease; for instance in the centre of the city the wetness is 27.39 and the mean LST is 46.21 °C, whilst in the 10 km buffer of the city the wetness decreases to 15.49, and the mean LST increased to 50.08 °C.

3.5.2. Surface temperature and brightness

The relationship between surface temperature and the brightness Index for LULC class is a strong positive correlation ($r = 0.75$; $p < 0.00001$). For instance, in the buffer zone of the city the Brightness is 77.32 and the mean surface temperature is 50.08 °C. Whilst, in the core of the city the Brightness is 69.14 and the surface temperature decreases to 46.21 °C.

3.5.3. Surface temperature and greenness

Between surface temperature and greenness Index a moderate negative correlation was found ($r = -0.39$; $p < 0.01$). The reason for this lack of correspondence is the lack of vegetation, especially during the dry season in the study area. However, in general areas of high greenness will exhibit lower surface temperature.

3.6. Spatial variation of LST in districts of the city

Figs. 6 and 7 indicate that in general old districts inside the 60 m street zone recorded low values of temperature. An Urban Cool Island effect is experienced in these areas with the exception of Qalat in the centre of the city which has a

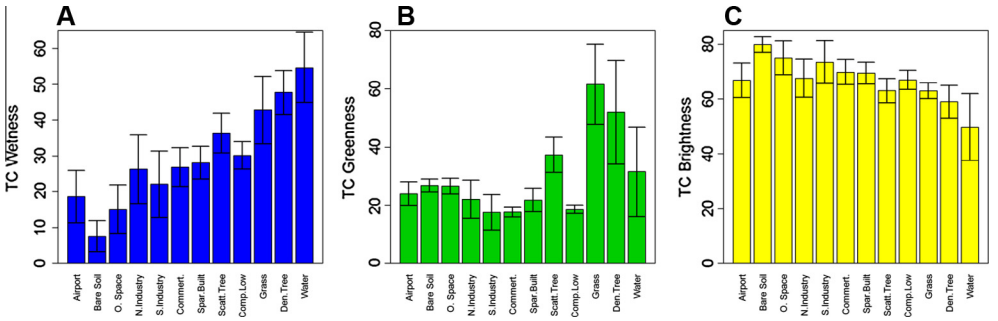

Fig. 4. Mean wetness, greenness and brightness for each LULC class during summer 2013.

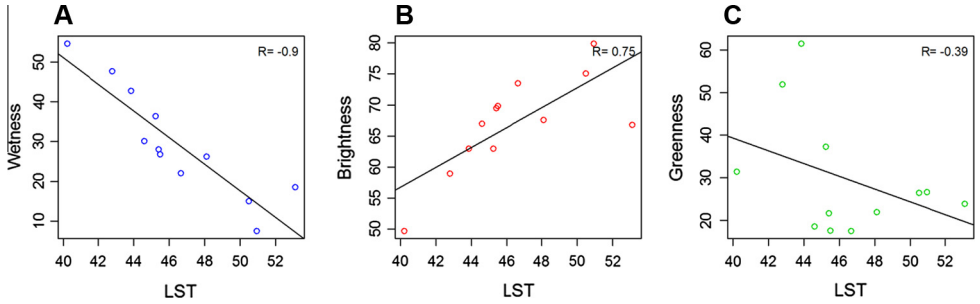

Fig. 5. Correlation coefficient between LST and wetness, brightness and greenness during summer 2013. Each plot represents a class of LULC.

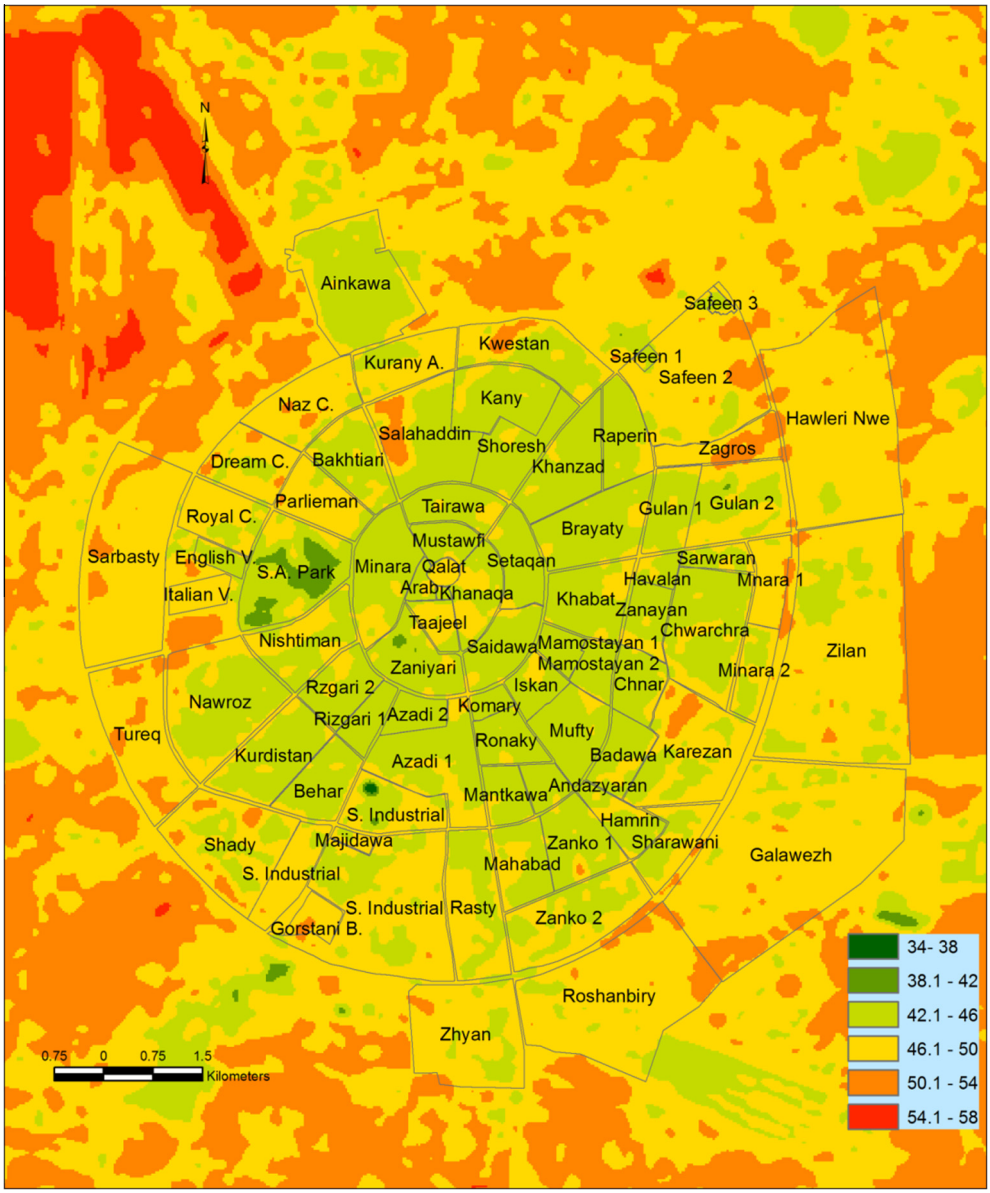

Fig. 6. LST of the districts of Erbil, during summer 2013, the data derived from composite image created from Landsat TIRS.

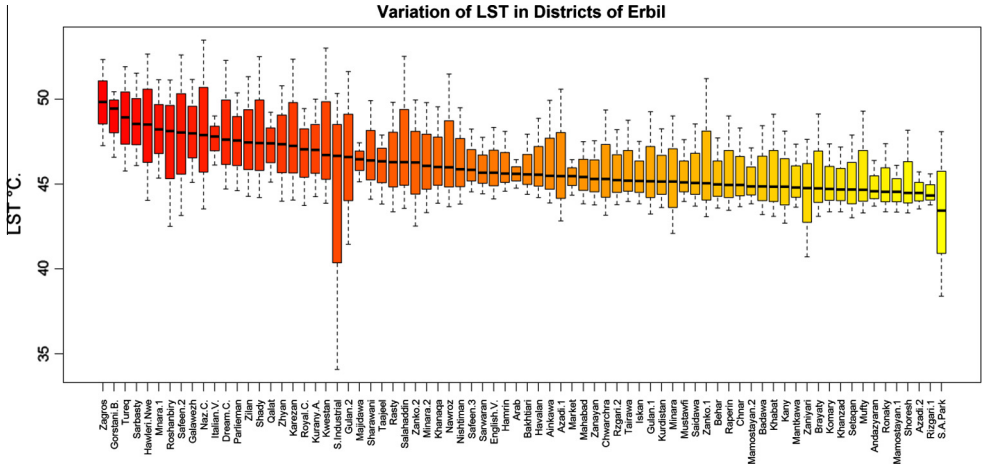

Fig. 7. LST of districts of Erbil during summer 2013.

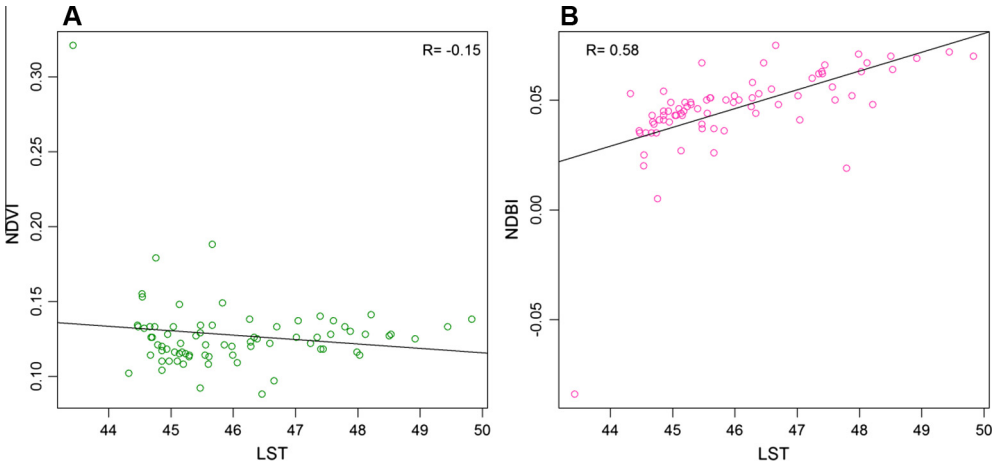

Fig. 8. Correlation coefficient of LST vs NDVI and NDBI during summer 2013. Each plot represents districts.

Table 3
Mean NDBI for different LULC class in the study area.

Class	Mean NDBI	SD NDBI
Bare soil	0.091	0.012
Built-up area	0.055	0.009
Water body	−0.061	0.048
Vegetation	−0.102	0.074

temperature of 47.4 ± 0.93 °C. The more modern built-up districts, which contain a wide open space areas, situated on the outskirts of the city, experienced a high average LST and low SUCI effect, for instance, Zagroz 49.83 ± 0.9 °C in the north east and Sarbasty 48.54 ± 1.04 °C in the west of the city (Fig. 6).

The highest average LST exists in Zagroz (49.83 ± 0.9 °C) and Tureq (48.92 ± 1.16 °C). Whilst the lowest average LST exists in Sami Abdurrahman Park, Rizgari 1 and Azadi 2, the LST was 43.43 ± 2.06, 44.32 ± 0.31 and 44.47 ± 0.44 °C for these areas respectively. On the other hand, the mean LST of some districts was normal and close to the average temperature of the city, for instance; Taajeel 46.34 ± 0.83 °C and Rasty 46.29 ± 1.31 °C.

3.7. Relationship between LST and built-up and vegetation index

Regression analysis was performed between mean LST and mean NDBI and NDVI index for each district of the city. Fig. 8 shows the results of these relationships, where each point on a scatter plot represents a district in the city.

The results indicate a strong positive relationship ($r = 0.58$; $p < 0.00001$) between mean LST and the NDBI. Meanwhile, a negligible inverse relationship ($r = -0.15$; $p < 0.00001$) is found, between surface temperature and the NDVI.

The results presented here show that the NDBI index is not congruent with the results from previous studies. In our study area the NDBI index cannot distinguish well between built-up areas and barren soil. Commonly, high NDBI refers to high built-up and low bare soil. Conversely, in this research, districts with high NDBI corresponding to low built-up density (Table 3), showed high temperature. For instance, the NDBI of Galawezh was 0.07 and its LST was 47.99 °C. In contrast, Azadi2 recorded 0.04 NDBI and 44.47 °C. The relationship between vegetation index and mean surface for each district was a negligible inverse relationship. For instance S.M. Park with the highest green index (0.32 NDVI) showed the lowest surface temperature 43.43 °C and Zaniyari with 0.18 NDVI recorded 44.76 °C.

In this study, we determined the spatial structure of LST and SUCI of Erbil city. The results indicate that during the daytime of summer, especially in the morning, the average surface temperature in built-up areas within the city boundaries is lower than the mean surface temperature in a 10 km non-urban reference zone around the city. The Surface Urban Cool Island Intensity of the central districts ranged from 3.5 to 4.6 °C. The results of this study indicate a daytime SUCI effect and they differ in this finding from other published studied of the UHI in densely vegetated regions (e.g. (Tran et al., 2006; Shahmohamadi et al., 2012; Dhorde and Dhorde, 2012). However, our results confirm results from previous studies in similar geographical areas which have pointed out the presence of a diurnal UCI effect in arid or semi-arid climates (e.g. (Frey et al., 2006; Li et al., 2011; Abdullah, 2012).

In the summer the climate of the city of Erbil is dry and hot. In such dry environments during the daytime the land surface on the outskirts of the city absorbs more heat than the urban area itself. Because the rural land surface is largely dry and barren in the dry season, it does not have large evaporation and transpiration effects to mitigate the temperature of the soil. Through examining the relationship between LST and SUCI with WI, GVI, BI and vegetation indices, it was found that a high bareness index is the most significant factor corresponding to an increase in LST. Likewise, the results indicate wetness is the second important factor in determining LST.

4. Conclusions

This investigation of the spatial distribution of surface temperature in Erbil city found that there is an inverse relationship between the building density and the surface temperature. Inside the city centre and high-density districts, the surface temperature is reduced in comparison to the surroundings of the city. However, on the outskirts of the city and in the modern districts with low-density housing construction, the surface temperature is increased. A daytime SUCI effect is diagnosed for the city centre and a SUHI effect for the low-density developments. Therefore, it will be possible in the future with a change from the rural to the compact low-rise areas, led to decrease a daytime surface temperature.

The research found a strong relationship between LST/SUCI with the wetness index and the Built-up index. Therefore, wetness and bareness are the main factors leading to the SUCI in the semi-arid environment of Erbil.

We conclude that in cities such as Erbil the surface wetness is the main determinant of the SUCI. This paper is limited to the spatial variation of the SUCI in the daytime during the dry season. Temporal variations including seasonal, diurnal and decadal variation of SUCI/SUHI in Erbil have been investigated by researchers and will be published in a forthcoming paper. Future studies on surface temperatures of cities in dry and semi-dry environments are required to confirm the results of this paper. Other research should focus on air temperature based Urban Heat Island exploration and the relationship between surface and air temperature UCI.

Acknowledgements

The authors would like to thank HCDP Scholarship and Soran University for their financial support of this research. Many thanks go to the USGS, for providing the research with Landsat 8 image of the case study area, free of charge. H. Balzter was supported by the Royal Society Wolfson Research Merit Award, 2011/R3 and the NERC National Centre for Earth Observation.

References

Abdullah, H. 2012. The use of Landsat 5 TM Imagery to detect urban expansion and its impact on land surface temperatures in the city of Erbil, Iraqi Kurdistan.

Amjed, A., Buchroithner, M., Prechtel, N. Object-oriented and decision tree classifications for LULC using Cosmo-SkyMed, QuickBird and LandSat 7 satellite data: an example of Erbil/Iraq.

Aufmuth, J.L. 2001. A comparison of the normalized difference and the tasseled cap vegetation indices: a case study of using satellite remote sensing imagery for assessment of environmental impact of a hydroelectric power project on the River Danube.

Baig, M.H.A., Zhang, L., Shuai, T., Tong, Q., 2014. Derivation of a tasselled cap transformation based on Landsat 8 at-satellite reflectance. Remote Sens. Lett. 5, 423–431.

Bajaj, D.N., Inamdar, A.B., Vaibhav, V. 2012. Temporal variation of Urban Heat Island using landsat data: a case study of Ahmedabad, India. In: 33rd Asian Conference on Remote Sensing 2012, ACRS 2012. vol. 1, pp. 797–804.

Cai, G., Du, M. 2009. Relationship between thermal inertia and urban heat sink in Beijing derived from Satellite images. pp. 1–5.

Chen, X., Zhao, H., Li, P., Yin, Z., 2006. Remote sensing image-based analysis of the relationship between urban heat island and land use/cover changes. Remote Sens. Environ. 104, 133–146.

Crist, E.P., Cicone, R.C., 1984. A physically-based transformation of Thematic Mapper data—The TM Tasseled Cap. IEEE Trans. Geosci. Remote Sens., 256–263

Dhorde, A., Dhorde, A., 2012. Surface Urban Heat Island. LAP Lambert Academic Publishing.

Farina, A. 2011. Exploring the relationship between land surface temperature and vegetation abundance for urban heat island mitigation in Seville, Spain.
Frey, C.M., Rigo, G., Parlow, E. Investigation of the daily Urban Cooling Island (UCI) in two coastal cities in an arid environment: Dubai and Abu Dhabi (UAE). City 81, p. 2.06.
Frey, C.M., Rigo, G., Parlow, E., Marçal, A. 2006. The cooling effect of cities in a hot and dry environment. pp. 169–174.
Gallo, K.P., Owen, T.W., 1999. Satellite-based adjustments for the urban heat island temperature bias. J. Appl. Meteorol. 38, 806–813.
Gillespie, A.R. 1986. Lithologic mapping of silicate rocks using TIMS.
Hartz, D., Prashad, L., Hedquist, B., Golden, J., Brazel, A., 2006. Linking satellite images and hand-held infrared thermography to observed neighborhood climate conditions. Remote Sens. Environ. 104, 190–200.
Hasan, T., 2006. Geographical analysis of the characteristics of the temperature in the Kurdistan Region of Iraq.
Jin, S., Sader, S.A., 2005. Comparison of time series tasseled cap wetness and the normalized difference moisture index in detecting forest disturbances. Remote Sens. Environ. 94, 364–372.
Karnieli, A., Agam, N., Pinker, R.T., Anderson, M., Imhoff, M.L., Gutman, G.G., Panov, N., Goldberg, A., 2010. Use of NDVI and land surface temperature for drought assessment: merits and limitations. J. Clim. 23, 618–633.
Kauth, R.J., Thomas, G., 1976. The tasselled cap–a graphic description of the spectral-temporal development of agricultural crops as seen by Landsat. p. 159.
KRSO, K., 2012. The number population of Erbil city (Urban – Rural) 2010.
Lazzarini, M., Marpu, P.R., Ghedira, H., 2013. Temperature-land cover interactions: the inversion of urban heat island phenomenon in desert city areas. Remote Sens. Environ. 130, 136–152.
Li, S., Mo, H., Dai, Y., 2011. Spatio-temporal pattern of Urban Cool Island Intensity and its eco-environmental response in Chang-Zhu-Tan Urban Agglomeration. Commun. Inf. Sci. Manage. Eng.
Li, Z., Becker, F., Stoll, M., Wan, Z., 1999. Evaluation of six methods for extracting relative emissivity spectra from thermal infrared images. Remote Sens. Environ. 69, 197–214.
Li, Z., Wu, H., Wang, N., Qiu, S., Sobrino, J.A., Wan, Z., Tang, B., Yan, G., 2013. Land surface emissivity retrieval from satellite data. Int. J. Remote Sens. 34, 3084–3127.
Liang, S., Shi, P., 2009. Analysis of the relationship between urban heat island and vegetation cover through Landsat ETM : a case study of Shenyang. pp. 1–5.
Liu, Q., Liu, G., Huang, C., Liu, S., Zhao, J., 2014. A tasseled cap transformation for Landsat 8 OLI TOA reflectance images. pp. 541–544.
Matson, M., Mcclain, E.P., McGinnis Jr., D.F., Pritchard, J.A., 1978. Satellite detection of urban heat islands. Mon. Weather Rev. 106, 1725–1734.
Meteorological and Seismological Department of Erbil Governorate. 2014. Elements Climatic Data of Erbil City.
Oke, T. 1987. Boundary layer climates.
Price, J.C., 1979. Assessment of the urban heat island effect through the use of satellite data. Mon. Weather Rev. 107, 1554–1557.
Rao, P., 1972. Remote sensing of urban heat islands from an environmental satellite. Bull. Am. Meteorol. Soc. 53, 647.
Schwarz, N., Schlink, U., Franck, U., Großmann, K., 2012. Relationship of land surface and air temperatures and its implications for quantifying urban heat island indicators—an application for the city of Leipzig (Germany). Ecol. Ind. 18, 693–704.
Shahmohamadi, P., Che-Ani, A., Sodoudi, S., Cubasch, U., 2012. Mitigating Urban Heat Island Effects in Tehran Metropolitan Area. INTECH Open Access Publisher.
Sharif, A. 1998. Climate of the Erbil Region.
Shigeta, Y., Ohashi, Y., Tsukamoto, O. 2009. Urban cool island in daytime—analysis by using thermal image and air temperature measurements. 29.
Sobrino, J.A., Jiménez-Muñoz, J.C., Paolini, L., 2004. Land surface temperature retrieval from LANDSAT TM 5. Remote Sens. Environ. 90, 434–440.
Srivastava, P., Majumdar, T., Bhattacharya, A.K., 2009. Surface temperature estimation in Singhbhum Shear Zone of India using Landsat-7 ETM thermal infrared data. Adv. Space Res. 43, 1563–1574.
Stathopoulou, M., Cartalis, C., 2007. Daytime urban heat islands from Landsat ETM and Corine land cover data: an application to major cities in Greece. Sol. Energy 81, 358–368.
Stewart, I.D., Oke, T.R., 2012. Local climate zones for urban temperature studies. Bull. Am. Meteorol. Soc. 93, 1879–1900.
Sun, D., Kafatos, M., 2007. Note on the NDVI-LST relationship and the use of temperature-related drought indices over North America. Geophys. Res. Lett. 34.
Todd, S., Hoffer, R., Milchunas, D., 1998. Biomass estimation on grazed and ungrazed rangelands using spectral indices. Int. J. Remote Sens. 19, 427–438.
Tran, H., Uchihama, D., Ochi, S., Yasuoka, Y., 2006. Assessment with satellite data of the urban heat island effects in Asian mega cities. Int. J. Appl. Earth Obs. Geoinf. 8, 34–48.
Ukwattage, N., Dayawansa, N. 2012. Urban Heat islands and the energy demand: an analysis for Colombo city of Sri Lanka using thermal remote sensing data.
USGS. 2013. Using the USGS Landsat 8 Product. 2015.
Voogt, J.A., Oke, T.R., 2003. Thermal remote sensing of urban climates. Remote Sens. Environ. 86, 370–384.
Watson, C., 2012. Analysis of Urban Heat Island Climates Along the I-85/I-40 Corridor in Central North Carolina. University of North Carolina, Greensboro.
Weng, Q., Lu, D., 2008. A sub-pixel analysis of urbanization effect on land surface temperature and its interplay with impervious surface and vegetation coverage in Indianapolis, United States. Int. J. Appl. Earth Obs. Geoinf. 10, 68–83.
Weng, Q., Lu, D., Schubring, J., 2004. Estimation of land surface temperature–vegetation abundance relationship for urban heat island studies. Remote Sens. Environ. 89, 467–483.
Wu, W., 2014. The generalized difference vegetation index (GDVI) for dryland characterization. Remote Sens. 6, 1211–1233.
Xu, S., 2009. An approach to analyzing the intensity of the daytime surface urban heat island effect at a local scale. Environ. Monit. Assess. 151, 289–300.
Yuan, F., Bauer, M.E., 2007. Comparison of impervious surface area and normalized difference vegetation index as indicators of surface urban heat island effects in Landsat imagery. Remote Sens. Environ. 106, 375–386.
Zha, Y., Gao, J., Ni, S., 2003. Use of normalized difference built-up index in automatically mapping urban areas from TM imagery. Int. J. Remote Sens. 24, 583–594.
Zhang, H., Qi, Z., Ye, X., Cai, Y., Ma, W., Chen, M., 2013. Analysis of land use/land cover change, population shift, and their effects on spatiotemporal patterns of urban heat islands in metropolitan Shanghai, China. Appl. Geogr. 44, 121–133.
Zhang, Z., Ji, M., Shu, J., Deng, Z., Wu, Y., 2008. Surface urban heat island in Shanghai, China: examining the relationship between land surface temperature and impervious surface fractions derived from Landsat ETM imagery. Int. Arch. Photogramm. Remote Sens. Spatial Inf. Sci. 6, 45, XXXVII (Pt.B8).